CORRIGENDUM

Pages 40, 44, and 45 of the article "The Generation and Propagation of a Nocturnal Squall Line. Part I: Observations and Implications for Mesoscale Predictability" by R. E. Carbone, J. W. Conway, N. A. Crook and M. W. Moncrieff, which appeared on pages 26–49 of the January 1990 issue of *Monthly Weather Review,* Vol. 118, No. 1, are reprinted in this corrigendum to correctly display Figs. 16, 19, and 21.

The corrected pages are also included as an insert to the January issue.

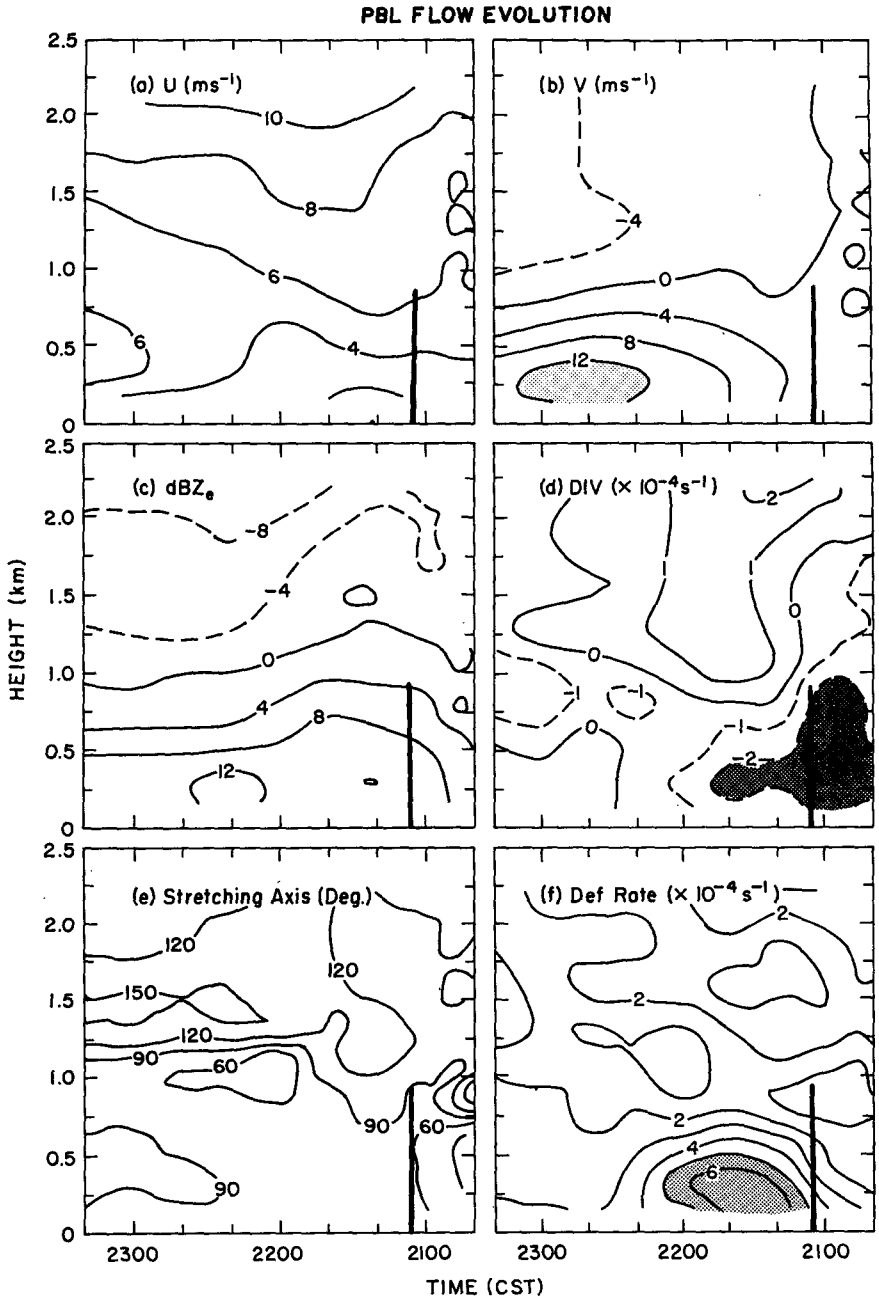

FIG. 16. Time–height series of kinematic fields as derived from harmonic (VAD) analyses at CP-4 prior to squall line development (a) u component, (b) v component, (c) reflectivity factor, (d) divergence, (e) axis of dilatation, (f) rate of deformation. Solid vertical line in each panel represents NPB passage at the radar (2105). Shaded regions denote same fields as in Fig. 16. Analysis frequency is 20 min.

c. The northward propagating boundary (NPB)

As discussed in section 3, the origin of the NPB appears to be related to convection in northern Oklahoma as illustrated by Figs. 9b and 9c. A small cold pool, located 60–120 km south-southeast of CP-4, trails the eastern part of the NPB when it is first detected by the radar. The western part of the NPB is trailed by warm, moist air and a small surge in southerly winds. Between 2030 and 2300, the NPB clearly becomes separated from the small cold pool as it propagates northwestward at a rate of 13 m s^{-1}. These observations suggest that transport of fluid from the cold pool may not have been necessary for the continued propagation of the

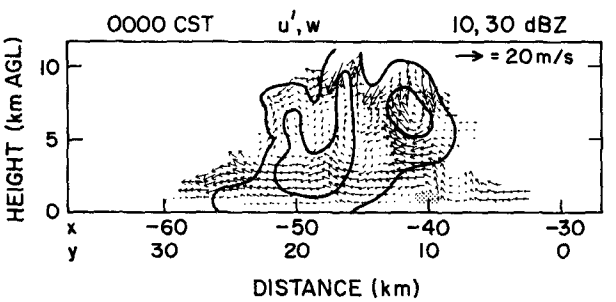

FIG. 19. (a) Dual-Doppler analysis horizontal cross section at 0000 CST and 0.75 km AGL with reflectivity contoured at 20, 30 dBZ_e (bold lines) and storm relative flow overlaid. Thin solid line represents the gust front as determined by 10 dBZ_e echo. Distance scale is relative to CP-4. (b) Same as (a) except for dBZ_e 5 km AGL. (c) Vertical cross-section depicting storm relative flow with contours at 10, 30 dBZ_e.

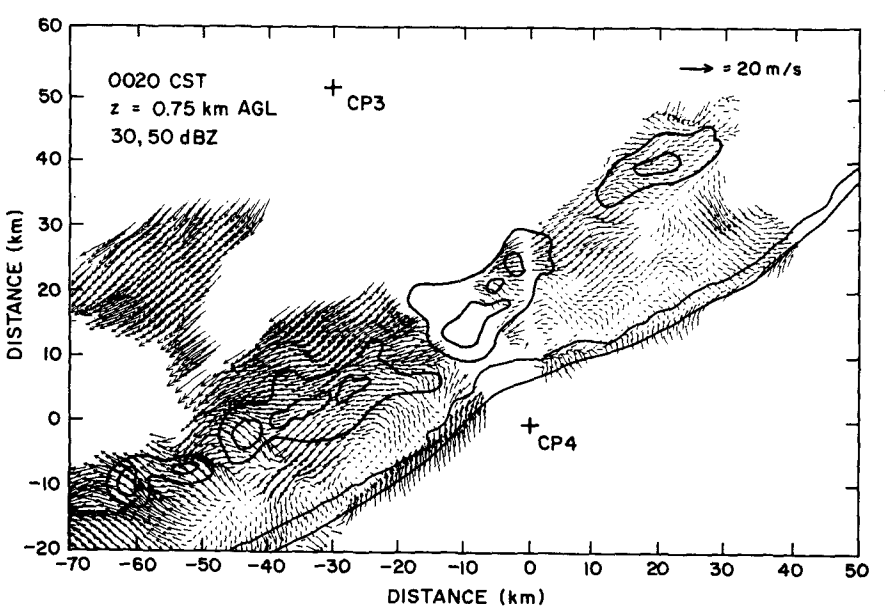

FIG. 20. Composite Doppler analysis showing storm relative flow over both eastern and western lobes (see Fig. 2) at 0020 and 0.75 km AGL with reflectivity contoured at 30, 50 dBZ_e.

the usual longevity and environmental stability criteria. Reflectivity and velocity structures aloft reveal that new cells no longer form over the gust front. Deep convection seems to consist of larger, more long-lived cells, roughly 15 km behind the gust front (as depicted in Fig. 23). There has been a rapid evolution from multicellular structure at 0000 to unicellular structure at 0020.

The vertical cross sections in Figs. 21 illustrate several features common to the squall line. The gust front is seen as a wavelike entity. Up to three wavelengths were observed in the PBL flow—coincident with and behind the gust front. The vertical resolution is insufficient to resolve extensive areas of motion toward the surface gust front in the cold air, but a flow reversal is observed in the head. In Fig. 21a, a secondary momentum surge is evident at $x = -43$. This may also be seen in Fig. 10c as a green line near the western edge of the radar echo. Front-to-rear flow-through is the dominant characteristic above 800 m and below 3 km. Deep convection is not obviously rooted in the lowest kilometer.

c. *The midlevel jet*

The rear-to-front midlevel jet (MLJ) is common to Figs. 21, 22 and 23. It is consistently observed near 5 km. Inflow toward the convective line is usually 6 to 8 m s^{-1}. The convective line seems to be sustained, in part, by the confluence of this midtropospheric inflow with the deeper, southerly inflow from the forward flank. In most regions the MLJ supplies a distinct secondary updraft. Less frequently (e.g., Fig. 23b), the MLJ appears to supply a rear flank downdraft.

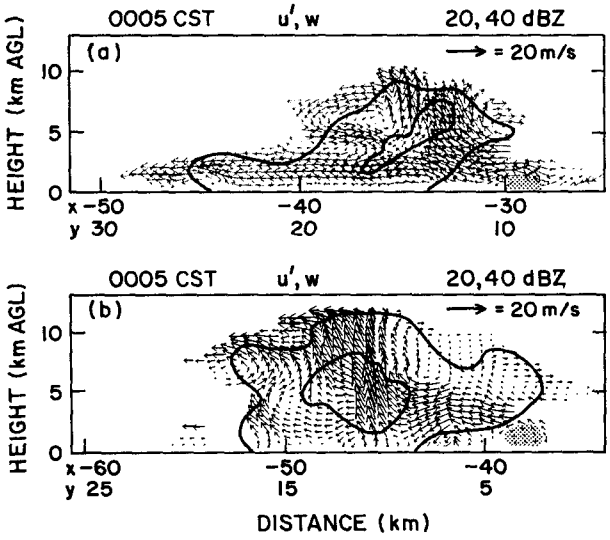

FIG. 21. Vertical cross-sections of u', w, dBZ_e through the squall line at 0005 showing storm relative flow. Contours are at 20, 40 dBZ_e and shaded region depicts the gust front.

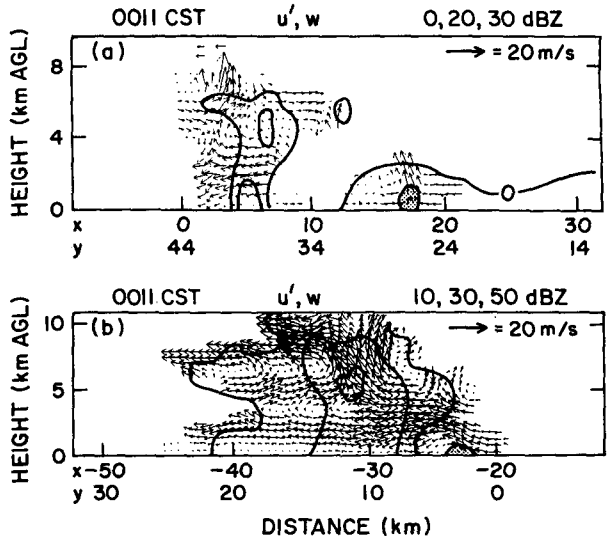

FIG. 22. As in Fig. 19 at 0011. In (a) contours of 0, 20, 30 dBZ_e are shown. In (b) 10, 30, 50 are shown.

Analysis of McPherson profiler data reveals a tendency for MLJ ascent of 5–10 cm s^{-1} as it approaches the squall line. This is calculated from the slope of the relative inflow axis as shown in Fig. 24.[4] The heights of inflow maxima relative to the convective line have been determined from the original numeric data. Subsequent application of the incompressible, two-dimensional mass-continuity equation allowed independent estimation of the mesoscale ascent rate. Contrary to most rear-to-front inflows (e.g., Zipser 1969; Houze 1977; Zipser and Matejka 1982; Leary and Rappaport 1987; Schmidt and Cotton 1985; Smull and Houze 1987), the MLJ appears to ascend on the mesoβ scale as air approaches the convective line.

Why does the MLJ ascend in this instance when the literature reveals numerous cases of mesoscale descent consistent with hydrostatic stability structure? A significant difference from other cases is the failure of this system to produce appreciable stratiform precipitation. Given that ascent is directed toward the convective line, trailing stratiform precipitation is not likely to be areally extensive. Notably, the source region for MLJ air is northwest—the direction of the dissipated primary squall line. Since convective overturning has diabatically heated that region, the concept of an ascending, moist, rear-to-front jet is qualitatively plausible. Examination of the 2100 and 0000 RSL soundings reveals 2°C sensible heating between 50 and 43 kPa and a moisture rise to near-saturation. The combined effects result in θ_e increase >3°K. A small amount of conditional instability is the net consequence of these changes. We hypothesize that this may be a common

[4] Note that MSL altitudes are given in Fig. 24.